

Spatial sensing of chemotactic gradients: A reaction-diffusion model

J. Krishnan
Electrical & Computer Engng
The Johns Hopkins University
Baltimore, MD 21218
krishnan@jhunix.hcf.jhu.edu

P.A. Iglesias
Electrical & Computer Engng
The Johns Hopkins University
Baltimore, MD 21218
pi@jhu.edu

L. Ma
Electrical & Computer Engng
The Johns Hopkins University
Baltimore, MD 21218
lma@jhu.edu

ABSTRACT

This paper analyzes a spatial gradient-sensing model for eukaryotic chemotaxis. The model is in the form of a reaction-diffusion system and comprises two enzymes A and I , whose production is mediated by the external signal S , as well as a response element R . This model possesses the property of adaptation to spatially homogeneous signals: the response to spatially homogeneous signals is independent of the concentration of the signal. The response to spatially inhomogeneous signals results in a spatially inhomogeneous response element. We consider the response of the cell in two cases: (a) A disk-shaped cell in 2-D in a constant gradient of chemoattractant and (b) A spherical cell in 3-D in a constant gradient of chemoattractant. The response of the cell is studied both analytically and numerically.

1. INTRODUCTION

Many different types of cells have the ability to direct their motion by external chemical concentration gradients. This process, known as chemotaxis, is exhibited in single-cell organisms such as *E. coli*, *D. discoideum* and leukocytes, as well as multicellular organisms such as *C. elegans*. It is most widely studied in the cells of the immune system and the social amoebae *D. discoideum*.

Mechanisms for detecting extra-cellular gradients can be divided broadly into two groups: *temporal* and *spatial* sensing. Organisms using temporal sensing compare the intensity of the external stimulus over time, as the organism moves from one location to another. Typically, cells that employ temporal sensing move randomly throughout their environment, altering their spatial orientation at random times. Depending on the gradient in their stimulus sensed over time, they alter the probability of changing directions. The resultant movement resembles a “biased” random walk in which the cell moves for longer intervals in the direction of desirable external stimuli. The best known organism using temporal sensing is the bacterium *E. coli* [4, 6]. Temporal sensing has also been postulated as the sensing scheme of the nematode *C. elegans* [16].

Some organisms are able to compare simultaneously the intensity of stimulus at different locations even while motionless, thus obtaining a profile of their environment — a process referred to as *spatial* or *gradient* sensing. These organisms then use this information to guide their movement. For example, it is known that human leukocytes can detect

a spatial gradient of γ -globulin [21].

Mechanisms for this gradient sensing have not been understood in as great a detail as those controlling temporal sensing. Several possibilities exist. In some systems, e.g. pheromone signaling in *S. cerevisiae* [3] receptors redistribute and thereby increase sensitivity at the anterior part of the cell.

In other organisms, such as *D. discoideum*, it has been demonstrated that receptors do not redistribute, but remain evenly distributed on the cell surface during reversals of polarity [20]. Similar experiments in neutrophils have also demonstrated no redistribution of receptors [18]. Thus, mechanisms must exist that can account for gradient sensing without receptor redistribution.

By measuring GFP-tagged CRAC binding to the membrane, it is possible to obtain a “readout” of cell polarization [14]. Using this technique, it has been possible to show that cells that are completely immobilized by inhibitors of actin polymerization, for example, latrunculin A, show an undiminished polarized response [14]. Thus, movement is not a necessary requirement for gradient sensing.

1.1 Adaptation

One common feature of many signaling systems exhibiting chemotaxis is the ability to adapt to different levels of external stimuli, so that it is primarily the gradient of the signaling molecule rather than the average signal value that determines the response. This allows, in part, for the great sensitivity observed by the cells.

Neutrophils, *D. discoideum*, and *S. cerevisiae* are able to detect and respond to extremely shallow chemoattractant gradients, as small as 2% across the cell’s diameter of approximately 10 μm . [11, 21, 19, 17] This level of sensitivity is observed when the mean concentration is near the apparent dissociation constant, though it does diminish for mean concentrations several orders of magnitude above or below this level.

2. GRADIENT SENSING: LOCAL ACTIVATION VS. GLOBAL INHIBITION

A hypothetical scheme for achieving gradient sensing has been postulated for more than a decade [5, 7, 15]. In this

scheme receptor occupancy generates both activation and inactivation signals. Two contrasting features of these signals dominate the response.

The first is that the time response of the activation signal is faster than that of the inhibitory signal. Thus, whenever there is an increase in receptor occupancy there will be a concomitant transient in response. However, as the inhibitory signal “catches up” to the activation signal, this response effect ceases. This scheme can explain the adaptation of the signals to homogeneous external concentrations.

The second main difference between the two signals is the fact that the excitatory signal is localized at or near the occupied receptor. The inhibitory signal, however, is allowed to distribute throughout the cell.

Conceptually, the scheme presented above is plausible. However, until recently, no formal verification has been conducted. In [10] a mathematical model of a gradient sensing mechanism using local excitation and global inhibition was presented. In the next section we show the basic ingredients.

3. MATHEMATICAL ANALYSIS OF THE MODEL

In this section we present the scheme of [10] that accounts for both spatial sensing and adaptation.

We assume that an response element is found in one of two states¹ *active* (R^*), or *inactive*; total concentration is R_T . Active excitory (A^*) and inhibitory (I^*) enzymes catalyze the activation and inactivation of the system. Activation of these enzymes is, in turn, regulated by receptor occupancy, which is proportional to the concentration of the local signaling molecule (S).

3.1 Adaptation

We assume that the ligand concentration is homogeneous. The equation describing the concentration of the active response element is

$$\frac{dR^*(t)}{dt} = -k_{-r}R^*(t)I^*(t) + k_r[R_T - R^*(t)]A^*(t) \quad (1)$$

leading to a steady-state, i.e. $\lim_{t \rightarrow \infty}$, concentration

$$\lim_{t \rightarrow \infty} R^*(t) =: \bar{R}^* = \frac{\bar{A}^*/\bar{I}^*}{K_R^{-1} + \bar{A}^*/\bar{I}^*} R_T \quad (2)$$

where $K_R = k_r/k_{-r}$ and \bar{R}^* is the steady-state level of the response element. Note that it is the *ratio* of enzyme concentrations that determines the steady-state value of activity. Perfect adaptation is preserved even if we allow these concentrations to vary with respect to the ligand concentration, provided that their dependence is the same. For example, assume that the two enzymes are regulated by receptor *occupancy*, which is in turn proportional to signal molecule concentration S according to

$$\frac{dI^*(t)}{dt} = -k_{-i}I^*(t) + k_i[I_T - I^*(t)]S$$

¹In the sequel, R^* , etc. refer to both the proteins and their concentrations.

and

$$\frac{dA^*(t)}{dt} = -k_{-a}A^*(t) + k_a[A_T - A^*(t)]S \quad (3)$$

After an initial transient, the active enzyme concentrations reach steady state

$$\lim_{t \rightarrow \infty} I^*(t) =: \bar{I}^* = \frac{S}{S + K_I^{-1}} I_T$$

and

$$\lim_{t \rightarrow \infty} A^*(t) =: \bar{A}^* = \frac{S}{S + K_A^{-1}} A_T$$

where $K_A = k_a/k_{-a}$, $K_I = k_i/k_{-i}$. These expressions can then be replaced in (2) to show the steady-state level of activity as a function of external signal concentration.

For perfect adaptation, this dependence should cancel out. This can be achieved provided that several assumptions hold. For example, suppose that $K_I^{-1} \gg S$, $K_A^{-1} \gg S$ so that the regulation of these two enzymes is in their linear region and suppose that $K_R^{-1} \gg \bar{A}^*/\bar{I}^*$. In this case we can check that \bar{R}^* will be independent of the signaling molecule concentration:

$$\frac{\bar{R}^*}{R_T} \approx K_R \frac{K_A}{K_I} \frac{A_T}{I_T} \quad (4)$$

and hence the system will exhibit perfect adaptation.

3.2 Spatial sensing.

So far we have only demonstrated that the scheme achieves perfect adaptation. But can it also perform spatial sensing? We now assume that the concentration of the two active enzymes A^* and I^* vary along the length of the cell, denoted x , with local ligand concentration $L(x)$. In turn, this gives rise to a local activity proportional to the ratio in enzyme concentrations

$$\lim_{t \rightarrow \infty} R^*(t, x) =: \bar{R}^*(x) \approx K_R \frac{\bar{A}^*(x)}{\bar{I}^*(x)} R_T$$

If, in the absence of ligand gradients, this dependence is the same for both enzymes, the steady state activity level, which is a function of the ratio between these two signals, will remain the same. Thus, adaptation — and more specifically, robust adaptation — will be preserved. This alone does not account for gradient sensing, but it does provide a means by which gradient sensing can be used.

Following a scheme outline by Parent and Devreotes [15] we postulate that these enzymes diffuse differently throughout the cell.

In particular, suppose that the activator enzyme cannot diffuse. In this case, the equation governing the activation of the activator enzyme is essentially (3), however, a spatial component is inherited by the external signal, now temporally *and* spatially dependent:

$$\frac{\partial A^*(t, x)}{\partial t} = -k_{-a}A^*(t, x) + k_a A_T S(x)$$

under the assumption that $A_T \gg A^*(t, x)$.

The steady-state solution is

$$\bar{A}^*(x) \propto S(x)$$

In contrast, we assume that the inhibitor diffuses easily:

$$\frac{\partial I^*(t, x)}{\partial t} = -k_{-i}I^*(t, x) + k_i I_T S(x) + D\nabla^2 I(t, x)$$

again, under the assumption that $I_T \gg I^*(t, x)$.

To solve this equation we assume that the external source varies linearly along the length of the cell:

$$S(x) = c_0 + c_1 x$$

where x is the normalized distance along the length of the cell. For boundary conditions we assume no flux at the two ends: $x \in \{0, 1\}$. In this case the steady-state solution is

$$\bar{I}^*(x) \propto \left(c_0 + c_1 \left(x - \frac{\sinh \sigma x}{\sigma} + \frac{\cosh \sigma x (\cosh \sigma - 1)}{\sigma \sinh \sigma} \right) \right)$$

where $\sigma = \sqrt{k_{-i}/D}$.

It follows that in the absence of a receptor occupancy gradient ($c_1 = 0$) the inhibitor level is constant. With a ligand gradient, the concentration gradient of the active inhibitor enzyme (and hence overall steady-state activity) will vary depending on the level of diffusion.

The response element is also assumed to be non-diffusible. Thus, proceeding as above leads to

$$\bar{R}^*(x) \propto \frac{c_0 + c_1 x}{c_0 + c_1 x + c_1 \left(\frac{\cosh \sigma x (\cosh \sigma - 1)}{\sigma \sinh \sigma} - \frac{\sinh \sigma x}{\sigma} \right)} \quad (5)$$

showing a spatial response when $c_1 \neq 0$.

The 1-dimensional analysis presented here is useful to demonstrate the suitability of the scheme of Levchenko and Iglesias [10]. However, in one dimension, the cell model does not differentiate between cell interior and membrane. For this reason, analysis for higher dimensions is desired.

4. ANALYSIS OF THE MODEL IN 2-D

In the previous section, the basic elements of the spatial gradient-sensing model were presented. As discussed previously, the response to spatially homogeneous external concentrations of the chemoattractant is independent of the concentration of the chemoattractant. If the external concentration of the chemoattractant is spatially varying, the response of the cell is dependent on the chemoattractant concentration profile.

While a 1-D model is useful for analyzing in detail to get some insight into the gradient sensing process, a realistic representation of the cell will require the extension of the above model to two and three dimensions. In this section we study a two-dimensional extension of the above model.

The specific problem we consider is the spatial response of the cell shaped as a disk, to a unidirectional external constant gradient of chemoattractant. Thus the above model is posed in the interior of the cylinder.

As discussed above, the main ingredients of the model are a long range inhibitor enzyme I , a short range non-diffusing

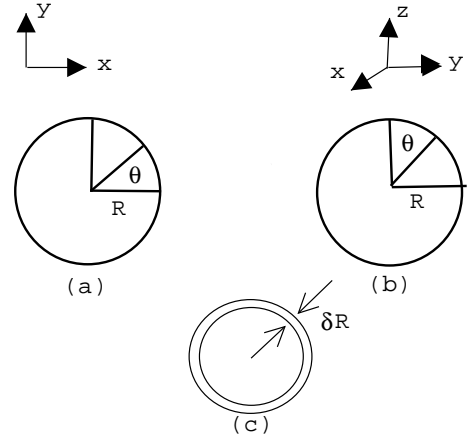


Figure 1: A schematic plot indicating the geometry of the cell: (a) Cell shaped as a disk of radius R ; θ is the polar angle. (b) Cell shaped as a sphere of radius R ; θ is the angle made by the radius vector with the z axis. (c) Schematic indicating that the response element is localized near the boundary of the cell in a ring of width δR .

(or weakly diffusing) activator enzyme A and a response element. In addition, there is another chemical S , the external signal, which mediates the activation of the enzymes A and I . The differential equations governing the concentrations of the species are, in dimensional form,

$$\begin{aligned} \frac{\partial I'}{\partial t} &= -k_{-i}I' + k_i S' + k_D \nabla^2 I' \\ \frac{\partial A'}{\partial t} &= -k_{-a}A' + k_a S' \\ \frac{\partial R'}{\partial t} &= -k_{-r}I'R' + k_r A'(R'_T - R') \end{aligned}$$

In the above S' denotes the signal concentration, while I' , A' and R' denote the concentrations of the inhibitor, activator and response element respectively. These equations are supplemented by “no-flux” boundary conditions at the boundary of the cell. In our case, we assume that the cell is in the shape of a circle of radius R , and that the signal S resides only close to the boundary of the cell boundary, specifically in the region $(1 - \delta)R \leq \hat{r} \leq R$. The set up in the 2-D case is depicted in Fig. 1(a) and 1(c).

At steady state the above model reduces to, in polar coordinates,

$$\begin{aligned} k_D \nabla^2 I' - k_{-i}I' + k_i S' H(\hat{r} - (1 - \delta)R) &= 0 \\ -k_{-a}A' + k_a S' H(\hat{r} - (1 - \delta)R) &= 0 \\ -k_{-r}I'R' + k_r A'(R'_T - R') &= 0 \end{aligned}$$

where

$$\nabla^2 = \frac{\partial^2}{\partial \hat{r}^2} + \frac{1}{\hat{r}} \frac{\partial}{\partial \hat{r}} + \frac{1}{\hat{r}^2} \frac{\partial^2}{\partial \theta^2}$$

In the above equations, $H(\cdot)$ is the Heaviside function, indicating that the activating signal is present only in a region near the outer boundary ($\hat{r} \geq (1 - \delta)R$). Smoother versions of the Heaviside function can also be employed.

The above equations can be cast in dimensionless form. Nondimensionalizing all concentrations by a quantity I_0 , and length by L (to be chosen), we obtain the following equations where $I = I'/I_0$, $A = A'/I_0$, $R^* = R'/I_0$, $r = \hat{r}/L$ and $R_T = R'_T/I_0$

$$\begin{aligned}\nabla^2 I - \frac{k_{-i}L^2}{k_D}I + \frac{k_iL^2}{k_D}SH(r - (1 - \delta)R/L) &= 0 \\ -k_{-a}A + k_aSH(r - (1 - \delta)R/L) &= 0 \\ -k_{-r}IR^* + k_rA(R_T - R^*) &= 0\end{aligned}$$

where

$$\nabla^2 = \frac{\partial^2}{\partial r^2} + \frac{1}{r} \frac{\partial}{\partial r} + \frac{1}{r^2} \frac{\partial^2}{\partial \theta^2}$$

We choose the length scale L such that $L^2k_{-i}/k_D = 1$. This is for convenience in the calculations later. The equations then become

$$\begin{aligned}\nabla^2 I - I + K_I SH(r - (1 - \delta)R/L) &= 0 \\ -k_{-a}A + k_aSH(r - (1 - \delta)R/L) &= 0 \\ -k_{-r}IR^* + k_rA(R_T - R^*) &= 0\end{aligned}$$

where $K_I = k_i/k_{-i}$. The no flux boundary condition is applied at $r = a = R(k_{-i}/k_D)^{1/2}$. We assume that $\delta \ll 1$.

The function $S(\theta)$ used in the above equation is the value at the boundary of the cell. This corresponds to the external concentration of the enzyme S at the boundary. We assume, for specificity, that a constant gradient of concentration exists in the y-direction and so outside the cell $S = \hat{f}_0 + \hat{f}_1 y$. Assuming the cell is centered at the origin the concentration at the boundary can be written as $S = f_0 + f_1 \sin(\theta)$, where $\hat{f}_0 = f_0$, and $\hat{f}_1 = R\hat{f}_1$.

We now proceed to solve the above equations. We note that when there is no signal, i.e. $S = 0$, the solution to the PDE governing the inhibitor profile is $I = 0$. The first step in solving the above equations, is to expand both I and S in a Fourier series in the angular variable. For the case under consideration, S has just two non-zero Fourier coefficients and hence so does I . We perform the expansion,

$$\begin{aligned}S(\theta) &= p_0 + \sum_{k=1}^{\infty} p_k \cos k\theta + q_k \sin k\theta \\ I(r, \theta) &= a_0 + \sum_{k=1}^{\infty} a_k \cos k\theta + b_k \sin k\theta\end{aligned}$$

In the above equations, the Fourier coefficients (a_k and b_k) of $I(r, \theta)$ are functions of r . Also, it trivially follows that $p_0 = f_0$, $q_1 = f_1$, and all other $p_k = 0$, $q_k = 0$. The ordinary differential equations governing the radial variation of the coefficients a_k , b_k are then obtained as

$$\begin{aligned}\frac{d^2 a_k}{dr^2} + \frac{1}{r} \frac{da_k}{dr} - \frac{k^2}{r^2} a_k - a_k &= -K_I p_k H(r - (1 - \delta)R/L) \\ \frac{d^2 b_k}{dr^2} + \frac{1}{r} \frac{db_k}{dr} - \frac{k^2}{r^2} b_k - b_k &= -K_I q_k H(r - (1 - \delta)R/L)\end{aligned}$$

These equations are supplemented by the conditions that a_k and b_k are finite at the origin, and that $da_k/dr = db_k/dr = 0$ at the outer boundary.

We start by noting that the only two equations of the above set, in which the right hand side is non-zero are the ones for a_0 and b_1 . Thus all the other coefficients are zero, as expected. We consider in turn, the equations for a_0 and b_1 . The equation for a_0 is

$$\frac{d^2 a_0}{dr^2} + \frac{1}{r} \frac{da_0}{dr} - a_0 = -K_I f_0 H(r - (1 - \delta)R/L)$$

This is an inhomogeneous linear ODE, the inhomogeneity being the factor on the right hand side. To construct a solution for this equation, we first obtain the solution to the corresponding homogeneous equation:

$$\frac{d^2 a_0}{dr^2} + \frac{1}{r} \frac{da_0}{dr} - a_0 = 0$$

Two linearly independent solutions to these equations are just the zeroth order modified Bessel functions, $y_1(r) = I_0(r)$ and $y_2(r) = K_0(r)$ [1, 2]. The particular solution for such an inhomogeneous second order linear differential equation is given by [2]

$$\begin{aligned}y_p(r) &= y_2(r) \int_0^r \frac{y_1(s)F(s)}{W(y_1(s), y_2(s))} ds \\ &\quad - y_1(r) \int_0^r \frac{y_2(s)F(s)}{W(y_1(s), y_2(s))} ds\end{aligned}$$

where $W(y_1, y_2)$ is the Wronskian of the two functions y_1 and y_2 (The Wronskian of two functions $y(x)$ and $z(x)$ is given by $W(y(x), z(x)) = y(x)z'(x) - z(x)y'(x)$). In this case, the Wronskian $W(I_0(s), K_0(s)) = -1/s$ [2]. Thus, the particular solution for a_0 is

$$\begin{aligned}y_p(r) &= K_0(r) \int_0^r s I_0(s) k_i f_0 H(s - (1 - \delta)R/L) ds \\ &\quad - I_0(r) \int_0^r s K_0(s) k_i f_0 H(s - (1 - \delta)R/L) ds\end{aligned}$$

It is worth noting that the particular solution above is non-zero only in the region where the signal concentration is non-zero. The complete solution for a_0 can be written as

$$a_0 = \hat{C}I_0(r) + \hat{D}K_0(r) + y_p(r)$$

where \hat{C} and \hat{D} are constants determined by imposing the boundary conditions. From the requirement of finiteness at the origin, it immediately follows that $\hat{D} = 0$. The coefficient \hat{C} is obtained from the no-flux boundary condition at the outer boundary. This results in

$$\hat{C} = -\frac{y'_p(R/L)}{I'_0(R/L)}$$

where y'_p is the derivative of y_p . Since I_0 is an increasing function of r and K_0 is a decreasing function of r , $y'_p \leq 0$, and so the constant \hat{C} is positive. Since $y_p(0) = 0$, $a_0(0) = \hat{C}I_0(0)$. The solution for a_0 is thus

$$a_0(r) = \hat{C}I_0(r) + y_p(r)$$

The equation for b_1 can be solved in exactly the same way.

The governing equation for b_1 is

$$\frac{d^2 b_1}{dr^2} + \frac{1}{r} \frac{db_1}{dr} - b_1 \left(1 + \frac{1}{r^2}\right) = -K_I f_1 H(r - (1 - \delta)R/L)$$

The corresponding homogeneous equation is

$$\frac{d^2 b_1}{dr^2} + \frac{1}{r} \frac{db_1}{dr} - b_1 \left(1 + \frac{1}{r^2}\right) = 0$$

Two linearly independent solutions of this equation are the modified Bessel functions of order 1, $y_1(r) = I_1(r)$, $y_2(r) = K_1(r)$. The Wronskian $W(y_1(s), y_2(s)) = -1/s$ [2]. Thus the particular solution for the inhomogeneous equation is

$$y_p(r) = K_1(r) \int_0^r s I_1(s) k_i f_1 H(s - (1 - \delta)R/L) ds - I_1(r) \int_0^r s K_1(s) k_i f_1 H(s - (1 - \delta)R/L) ds$$

Again the general solution for this equation is

$$b_1(r) = \hat{G} I_1(r) + \hat{H} K_1(r) + y_p(r)$$

As before, we have, by imposing the boundary conditions,

$$\begin{aligned} \hat{H} &= 0 \\ \hat{G} &= -\frac{y_p'(R/L)}{I_1'(R/L)} \end{aligned}$$

Finally, the inhibitor concentration is obtained as

$$I^*(r, \theta) = a_0(r) + b_1(r) \sin \theta$$

The functions $a_0(r)$ and $b_1(r)$ have been calculated above. This expression gives the inhibitor concentration in the entire cell. The activator and response element are localized to the region where the signal is present. The concentrations of the activator and response element are given by

$$A^*(\theta) = \frac{k_a}{k_{-a}} S(\theta) = \frac{k_a}{k_{-a}} (f_0 + f_1 \sin \theta)$$

and

$$R^* = \frac{k_r A^*}{k_{-r} I^* + k_r A^*} R_T$$

4.1 Relationship to adaptation and gradient sensing

We now analyze the results of the previous section in a little more detail. It is known that when the cell is presented with a spatially homogeneous signal, its response is independent of the magnitude of the signal. This property is known as adaptation. We show below that the concentration of the response element R^* in the presence of a spatially uniform external signal is independent of the magnitude of the external signal. This, in turn, is a simple consequence of the linearity of the equations governing A^* and I^* .

A spatially homogeneous external concentration of chemoattractant can be described in the above calculations by setting $f_1 = 0$ and keeping f_0 constant. The concentrations of

the inhibitor, activator and response element are given by

$$\begin{aligned} I^*(r, \theta) &= a_0(r) \\ A^*(\theta) &= \frac{k_a}{k_{-a}} S(\theta) = \frac{k_a}{k_{-a}} f_0 \end{aligned}$$

and

$$R^* = \frac{k_r A^*}{k_{-r} I^* + k_r A^*} R_T = \frac{k_r A^* / I^*}{k_{-r} + k_r A^* / I^*} R_T$$

We see that the activator concentration (in the region in which it is present) depends linearly on the concentration of the external signal (which is constant). We also see that the concentration of the response element depends on the ratio of the activator and inhibitor concentrations A^*/I^* . The inhibitor concentration is given by

$$I^*(r, \theta) = a_0(r) = \hat{C} I_0(r) + y_p(r)$$

where

$$\begin{aligned} y_p(r) &= K_0(r) \int_0^r s I_0(s) k_i f_0 H(s - (1 - \delta)R/L) ds \\ &\quad - I_0(r) \int_0^r s K_0(s) k_i f_0 H(s - (1 - \delta)R/L) ds \end{aligned}$$

and

$$\hat{C} = -\frac{y_p'(R/L)}{I_0'(R/L)}$$

It is easy to see from the above equations that the particular solution $y_p(r)$ depends on f_0 linearly. Furthermore, the constant \hat{C} also depends on f_0 linearly, since the derivative of y_p depends on f_0 linearly. Thus the overall dependence of $a_0(r)$ on f_0 is linear (i.e. $a_0(r)$ is proportional to f_0). Hence the ratio A^*/I^* is independent of f_0 . It immediately follows that the concentration R^* of the response element is independent of f_0 .

When f_0 and f_1 are non-zero, the response of the cell is also dependent on θ . The functions $a_0(r)$ and $b_1(r)$ are positive functions of r . The input has a maximum at $\theta = 0$ and a minimum at $\theta = \pi$. We find that the response element also has the same behavior. A plot of the activator, inhibitor and response element concentrations for an input with $f_0 = 1$, $f_1 = 1/2$ is shown in the next section. Note that the activator and response element are localized near the boundary of the cell.

5. ANALYSIS OF THE MODEL IN 3-D

We now consider the same model in 3-D, i.e. we model the cell as a sphere in a unidirectional gradient of chemoattractant, and determine its response.

The setting is very similar to that of the previous section: the cell is modeled as a sphere of radius R centered at the origin, and the external concentration of the chemoattractant is given by $\hat{f}_0 + \hat{f}_1 z$ which corresponds to a gradient in the z -direction. This means that at the surface of the sphere, the concentration of the chemoattractant can be written as $f_0 + f_1 \cos \theta$, with $f_0 = \hat{f}_0$ and $f_1 = R \hat{f}_1$.

Since there is symmetry with respect to the azimuthal angle ϕ , the concentrations of the various species are independent of ϕ , and dependent only on the radial co-ordinate r and the polar angle θ (see Fig. 1(b)) Scaling the equations just as before, we obtain at steady state

$$\begin{aligned}\nabla^2 I - I + K_I S H(r - (1 - \delta)R/L) &= 0 \\ -k_{-a}A + k_a S H(r - (1 - \delta)R/L) &= 0 \\ -k_{-r}IR^* + k_r A(R_T - R^*) &= 0\end{aligned}$$

where, in this case:

$$\nabla^2 = \frac{\partial^2}{\partial r^2} + \frac{2}{r} \frac{\partial}{\partial r} + \frac{1}{r^2 \sin \theta} \frac{\partial}{\partial \theta} \sin \theta \frac{\partial}{\partial \theta}$$

As in the two-dimensional case, no flux boundary conditions are imposed at the boundary of the sphere.

The solution procedure is very similar to that before. First we take care of the angular dependence of the solution. Since the signal S has angular components comprising of 1 and $\cos \theta$ which are also the first two spherical harmonics, we assume that the inhibitor concentration can be written as

$$I^*(r, \theta) = a_0 + a_1 \cos \theta$$

The governing differential equation for a_0 is

$$\frac{d^2 a_0}{dr^2} + \frac{2}{r} \frac{da_0}{dr} - a_0 = -f_0 K_I H(r - (1 - \delta)R/L)$$

This is solved exactly as before. The corresponding homogeneous equation is

$$\frac{d^2 a_0}{dr^2} + \frac{2}{r} \frac{da_0}{dr} - a_0 = 0$$

Two linearly independent solutions to this equation are the so-called modified spherical Bessel functions $y_1(r) = i_0(r)$, $y_2(r) = k_0(r)$ [2] where the modified spherical Bessel functions are related to modified Bessel functions as

$$\begin{aligned}i_0(r) &= \sqrt{\pi/2r} I_{1/2}(r) \\ k_0(r) &= \sqrt{\pi/2r} K_{1/2}(r)\end{aligned}$$

and, in general

$$\begin{aligned}i_n(r) &= \sqrt{\pi/2r} I_{n+1/2}(r) \\ k_n(r) &= \sqrt{\pi/2r} K_{n+1/2}(r)\end{aligned}$$

The Wronskian of functions i_n and k_n for all n are given by [2]

$$W(i_n(r), k_n(r)) = -\frac{1}{r^2}$$

Thus, the particular solution for the equation for a_0 is given by

$$\begin{aligned}y_p(r) &= k_0(r) \int_0^r s^2 i_0(s) k_i f_0 H(s - (1 - \delta)R/L) ds \\ &\quad - i_0(r) \int_0^r s^2 k_0(s) k_i f_0 H(s - (1 - \delta)R/L) ds\end{aligned}$$

Proceeding as in the 2-D case, the solution for a_0 is written as

$$a_0(r) = C_1 i_0(r) + C_2 k_0(r) + y_p(r)$$

where $C_2 = 0$ from the requirement of finiteness at the origin, and C_1 is given by,

$$C_1 = -\frac{y'_p(R/L)}{i'_0(R/L)}$$

The governing equation for a_1 is

$$\frac{d^2 a_1}{dr^2} + \frac{2}{r} \frac{da_1}{dr} - a_1 \left(1 + \frac{2}{r^2}\right) = -f_1 K_I H(r - (1 - \delta)R/L)$$

The corresponding homogeneous equation is

$$\frac{d^2 a_1}{dr^2} + \frac{2}{r} \frac{da_1}{dr} - a_1 \left(1 + \frac{2}{r^2}\right) = 0$$

for which two linearly independent solutions are the modified spherical Bessel functions of order 1, $y_1(r) = i_1(r)$, $y_2(r) = k_1(r)$. The particular solution is written as

$$\begin{aligned}y_p(r) &= k_1(r) \int_0^r s^2 i_1(s) k_i f_1 H(s - (1 - \delta)R/L) ds \\ &\quad - i_1(r) \int_0^r s^2 k_1(s) k_i f_1 H(s - (1 - \delta)R/L) ds\end{aligned}$$

The complete solution for a_1 is thus written as

$$a_1(r) = G i_1(r) + H k_1(r) + y_p(r)$$

where

$$H = 0$$

and

$$G = -\frac{y'_p(R/L)}{i'_1(R/L)}$$

The inhibitor concentration profile is now given by

$$I^*(r, \theta) = a_0(r) + a_1(r) \cos \theta$$

The concentrations of the activator and the response element are, once again

$$\begin{aligned}A^* &= \frac{k_a}{k_{-a}} S \\ R^* &= \frac{k_r A^*}{k_{-r} I^* + k_r A^*} R_T\end{aligned}$$

Thus, the overall approach to obtaining the profile in 3-D is very similar to that in 2-D. We again obtain explicit expressions for the concentration profiles of the inhibitor, activator and response element. The activator and response element are localized in a region near the boundary of the sphere. Just like before, we can demonstrate the adaptation property of the cell-sensing mechanism to homogeneous external chemoattractant concentrations.

6. NUMERICAL SIMULATIONS

In this section we shall indicate some of the numerical calculations performed with this model in 2-D to obtain the concentration profiles of the activator, inhibitor and response element concentration profiles.

All simulations are performed for the case where the cell is shaped as a disk of radius R . The values of the various rate constants are as follows: $k_r = k_{-r} = 1$, $k_a = k_{-a} = 2$, $k_i = k_{-i} = 1$ (units for k'_i s and k'_a s are in inverse seconds, those of k_r and k_{-r} are in inverse seconds, inverse nM; and $k_D = 100\mu\text{m}^2/\text{s}$. The radius of the cell is taken to be $10\mu\text{m}$ and the thickness of the annular ring in which the activator and inhibitor reside is $0.5\mu\text{m}$.

The first case we consider is the effect of a uniform external concentration of chemoattractant. The first column of Fig. 2 shows respectively the concentration profiles of the inhibitor, activator and response element. We see that there is no variation in the angular direction. Now, if we increase the external concentration of the chemoattractant, we see in the third column of Fig. 2 that the new response element concentration is the same as before, thus illustrating perfect adaptation. The steady activator and inhibitor concentrations are also shown in the third column and it is evident that they have changed. The second column shows instantaneous profiles of the inhibitor, activator and response element at an intermediate time.

In Fig. 3 we show the activator, inhibitor and response element concentrations when the external concentration of the signal is inhomogeneous. The first row shows the instantaneous concentration profiles at an intermediate time, and the second row shows the steady state values. The plot below (c) shows the external concentration profile of the signal. This, in turn, is obtained by finding the concentration profile external to the cell corresponding to a localized source of signal.

Finally, in Fig. 4 we show the inhibitor and response element profiles arising from an external signal profile given by $f_0 + f_1 \sin \theta$ which in turn corresponds to a linear concentration profile with a constant gradient in the y-direction.

7. CONCLUSIONS

In this paper we have demonstrated that the mathematical model of gradient sensing formulated by Levchenko and Iglesias will work for cell models of both two and three dimensions. The biological plausibility of the model is detailed in [10] for both amoeba and leukocytes.

It should be stressed that the model presented here is only one component of the whole signaling cascade involved in eukaryotic gradient sensing. One feature it fails to show is the large gains in sensitivity that are seen experimentally. In fact, as seen in (5) in the one-dimensional case, the response element's concentration is of the form of $\bar{R}^*(x) = 1/(1 + f(x))$ where $f(x)$ is a non-negative function of the spatial dimension. Thus, the difference in activity between the front and rear of this model of the cell is always *lower* than that of the external chemoattractant gradient. Mathematical models that account for this high amplification ex-

ist [12, 13], however, neither of these achieves its amplification at the same time as it achieves perfect adaptation. A model of a system that accounts for gain amplification is presented in [8]. That it can be appended to the gradient sensing mechanism is demonstrated in [10]. Thus, the gradient sensing mechanism postulated here can act as a "control module" in the sense discussed in [9].

8. ACKNOWLEDGMENTS

This work was supported in part by the National Science Foundation, under grant DMS-0083500, and the Whitaker Foundation. Conversations with Peter Devreotes and Andre Levchenko are gratefully acknowledged.

9. REFERENCES

- [1] M. Abramowitz and I.E. Stegun. *Handbook of Mathematical Functions*. Dover Publications, New York, 1974.
- [2] G.B. Arfken and H.J. Weber. *Mathematical Methods for Physicists*. Academic Press, Inc, San Diego, USA, 1995.
- [3] K.R. Ayscough and D.G. Drubin. A role for the yeast actin cytoskeleton in pheromone receptor clustering and signalling. *Curr. Biol.*, 8(16):927–930, 1998.
- [4] H.C. Berg and D.A. Brown. Chemotaxis in *Escherichia coli* analysed by three-dimensional tracking. *Nature*, 239(5374):500–504, Oct. 27 1972.
- [5] P.N. Devreotes and S.H. Zigmond. Chemotaxis in eukaryotic cells: A focus on leukocytes and *dictyostelium*. *Ann. Rev. Cell Bio.*, 4:649–686, 1988.
- [6] D.B. Dusenberry. Spatial sensing of stimulus gradients can be superior to temporal sensing for free-swimming bacteria. *Biophys. J.*, 74(5):2272–2277, May 1998.
- [7] P.R. Fisher. Pseudopodium activation and inhibition signals in chemotaxis by *Dictyostelium discoideum* amoebae. *Semin. Cell Biol.*, 1:87–97, 1990.
- [8] P.A. Iglesias and A. Levchenko. Spatial sensing in *Dictyostelium*: Amplification through saturating nonlinearities. In *International Conf. Systems Biology*, Tokyo, 154–159, November 2000.
- [9] D.A. Lauffenburger. Cell signaling pathways as control modules: Complexity for simplicity? *Proc. Natl. Acad. Sci. USA*, 97(9):4649–4653, Apr. 25 2000.
- [10] A. Levchenko and P.A. Iglesias. Models of eukaryotic gradient sensing: applications to chemotaxis of amoebae and neutrophils. Submitted, April 2001.
- [11] J.M. Mato, A. Losada, V. Nanjundiah, and T.M. Konijn. Signal input for a chemotactic response in the cellular slime mold *Dictyostelium discoideum*. *Proc. Natl. Acad. Sci. USA*, 72(12):4991–4993, December 1975.
- [12] H. Meinhardt. Orientation of chemotactic cells and growth cones: Models and mechanisms. *J. Cell Sci.*, 112:2867–2874, August 1999.

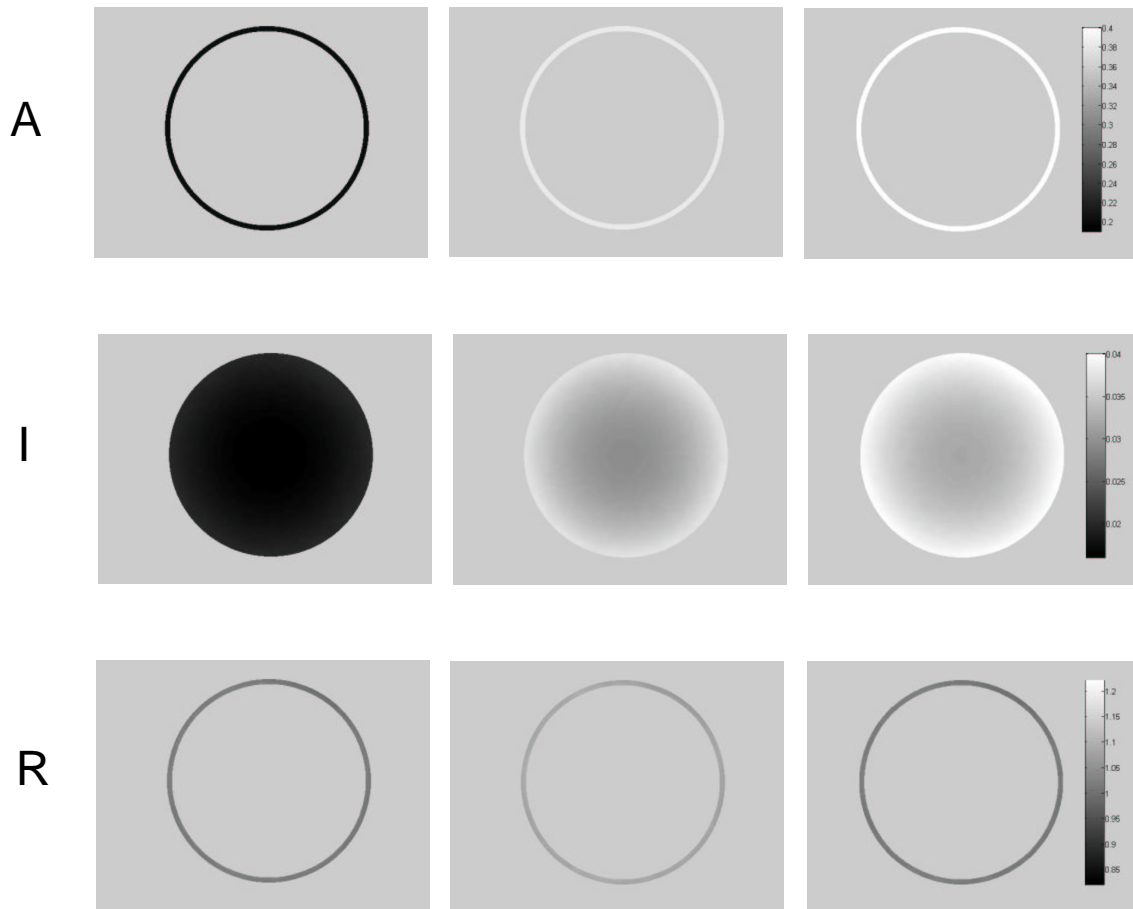


Figure 2: The response of the cell owing to a step change in the homogeneous external concentration. (a) The initial activator, inhibitor and response element concentrations, corresponding to $S = 0.2$ nM. (b) The concentration profiles at an intermediate time when the external concentration level is changed to $S = 0.4$ nM. (c) The final steady-state concentrations owing to the external signal $S = 0.4$ nM. Parameters are as indicated in the text.

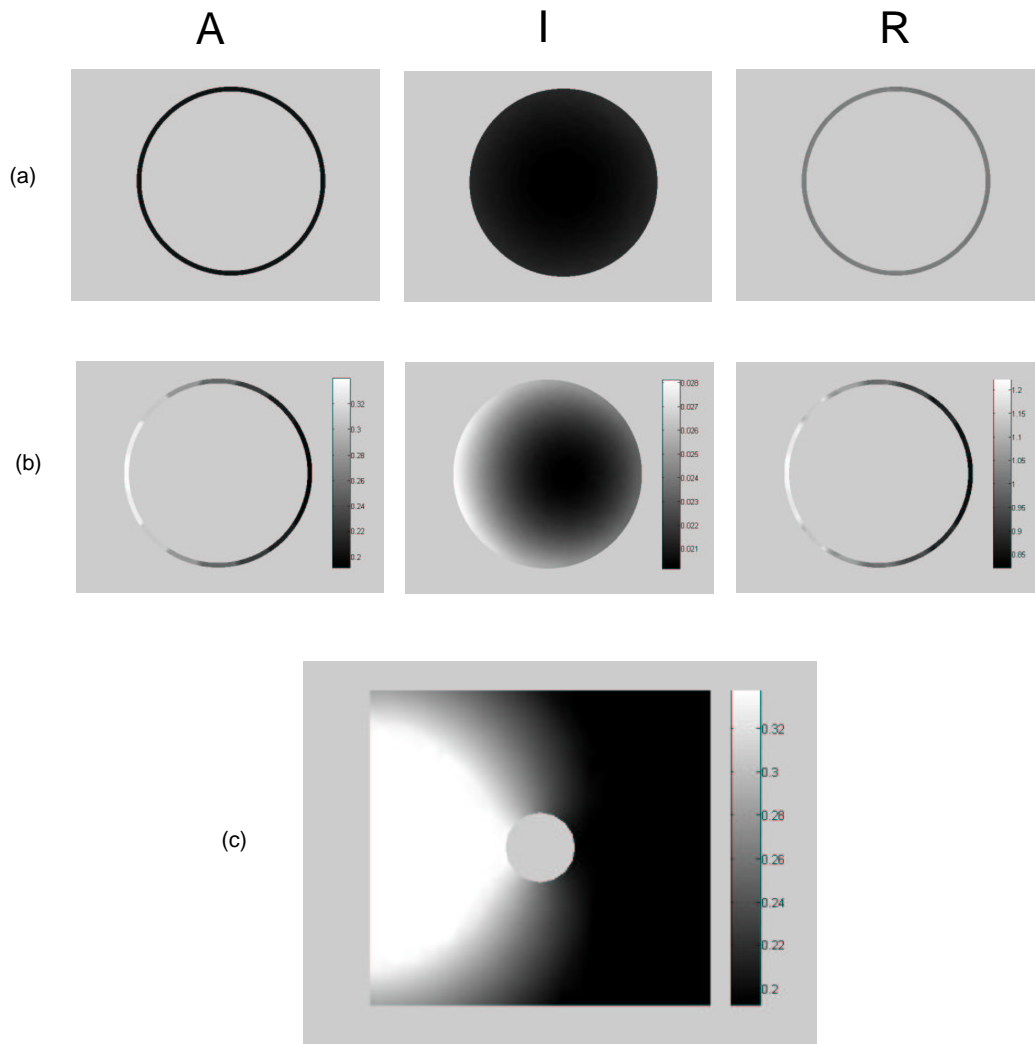


Figure 3: The response of the cell to an external inhomogeneous profile of S . This profile is that of an external point concentration and is shown in (c). The initial (a) and final (b) concentrations of all three species are shown. It should be noted that all three species show a spatial response.

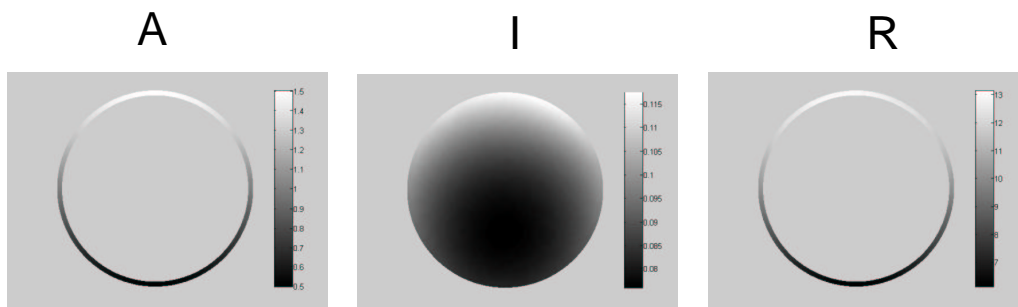


Figure 4: The steady state concentration profile to a uniform gradient imposed in the y -direction. $S(\theta) = f_0 + f_1 \sin \theta$ where $f_0 = 0$ and $f_1 = 1/2$ nM.

- [13] A. Narang and D. Lauffenburger. A mathematical model for a lipid-based signal transduction process for directional sensing. Unpublished abstract.
- [14] C.A. Parent, B.J. Blacklock, W.M. Froehlich, D.B. Murphy, and P.N. Devreotes. G protein signaling events are activated at the leading edge of chemotactic cells. *Cell*, 95(1):81–91, 1998.
- [15] C.A. Parent and P.N. Devreotes. A cell's sense of direction. *Science*, 284:765–770, 1999.
- [16] J.T. Pierce-Shimomura, T.M. Morse, and S.R. Lockery. The fundamental role of pirouettes in *Caenorhabditis elegans* chemotaxis. *J. Neurosci.*, 19(21):9557–9569, Nov. 1 1999.
- [17] I.H. Segel. *Enzyme Kinetics: Behavior and Analysis of Rapid Equilibrium and Steady State Enzyme Systems*. Wiley Classics Library ed., New York, NY, 1993.
- [18] G. Servant, O.D. Weiner, P. Herzmark, T. Balla, J.W. Sedat, and H.R. Bourne. Polarization of chemoattractant receptor signaling during neutrophil chemotaxis. *Science*, 287:1037–1040, Feb. 11 2000.
- [19] R.T. Tranquillo, D.A. Lauffenburger, and S.H. Zigmond. A stochastic model for leukocyte random motility and chemotaxis based on receptor binding fluctuations. *J. Cell Biology*, 106(2):303–309, February 1988.
- [20] Z. Xiao, N. Zhang, D.B. Murphy, and P.N. Devreotes. Dynamic distribution of chemoattractant receptors in living cells during chemotaxis and persistent stimulation. *J. Cell Biology*, 139(2):365–374, Oct. 20 1997.
- [21] S.H. Zigmond. Ability of polymorphonuclear leukocytes to orient in gradients of chemotactic factors. *J. Cell Biology*, 75(2):606–616, November 1977.